Glass Transitions of Polymers with Compressed Fluid Diluents: Type II and III Behavior

P. D. Condo, D. R. Paul, and K. P. Johnston*

Department of Chemical Engineering, The University of Texas at Austin, Austin, Texas 78712

*Received June 3, 1993; Revised Manuscript Received October 22, 1993**

ABSTRACT: The effect of CO_2 solubility on T_g versus CO_2 partial pressure behavior is presented for poly(methyl methacrylate) (PMMA), polystyrene (PS), and a random copolymer of the two with 60% by weight methyl methacrylate. Two new features of T_g versus pressure behavior have been discovered experimentally, confirming previous theoretical predictions (Condo, et al. *Macromolecules* **1992**, *25*, 6119). The results for the copolymer, poly(methyl methacrylate-*co*-styrene) (SMMA60), reveal a novel "z-shape" in the T_g behavior as a function of pressure, including a narrow pressure region in which three glass transitions take place upon changing the temperature isobarically (type III behavior). In contrast, only one glass transition temperature for each pressure is present for PS, without an extremum (type II behavior). The results are modeled accurately with lattice fluid theory and explained in terms of the combined effects of pressure and temperature on the solubility of the diluent in the polymer.

Introduction

Compressed fluids, including supercritical fluids, have been used in polymer separation and purification processes such as extraction[1–4] and fractionation.[1,5] These fluids have also been utilized to facilitate impregnation of polymers with additives,[6] and to condition polymer membranes.[7,8] In the Unicarb spray painting process,[9] CO_2 is used as a thinner in place of hydrocarbons, to decrease VOC emissions by up to 75%. Several innovative processes have been developed which utilize compressed fluids in the production of advanced polymeric materials such as microcellular foams,[10,11] gels,[12] fibers,[13–15] and microparticles.[11,13–17] CO_2 is a desirable solvent for polymer processing since it is nontoxic, nonflammable, and inexpensive. After processing, CO_2 removal from the polymer is accomplished simply by decreasing the pressure.

In many of the above processes, the plasticization of the polymer by the compressed fluid plays an important role. One way to address plasticization is to study the effect of the compressed fluid on the T_g behavior of the polymer. However, very little T_g data are available in the temperature and pressure regions of interest. Recently, an experimental technique has been developed to measure the creep compliance for the determination of the glass transition of polymers in the presence of compressed fluids.[18] This technique offers important advantages over other methods.[19,20] Measurements are made at constant temperature and pressure, allowing establishment of equilibrium sorption of diluent in the polymer. In contrast, the temperature is varied in differential scanning calorimetry (DSC) which can cause unwanted desorption of the diluent.[19] Another advantage is that the T_g is easily identifiable since the creep compliance changes by orders of magnitude. For measurements of T_g from discontinuities in sorption and dilation isotherms, changes are slight, leading to large uncertainties.[20]

A model has been developed to predict the effect of compressed fluid diluents on the T_g behavior of polymers as a function of pressure and diluent concentration.[21] New regions of temperature and pressure were explored, revealing three novel types of T_g behavior as a function of pressure. Characteristic features of the various types are shown in Figure 1. A new phenomenon, retrograde vitrification, was discovered where a polymer undergoes a liquid to glass transition by increasing the temperature. For example, this retrograde behavior is evident in a type IV system at 40 bar. Also, a pressure maximum is present at 52 bar. Type IV behavior has been confirmed experimentally for PMMA by using CO_2 as a diluent.[18,22] An important practical result is that polymers may be plasticized at lower temperatures and pressures than thought previously. Indeed, microcellular foams may be produced by depressurizing PMMA containing CO_2 at room temperature.[10]

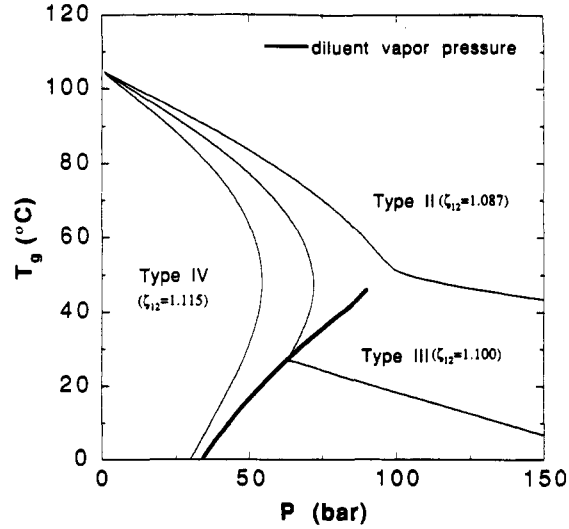

Figure 1. Characteristic features of polymer T_g behavior predicted as a function of diluent pressure for various values of the polymer–diluent interaction parameter, ζ_{12}. Pure component parameters are for PMMA and CO_2 with a pure PMMA T_g of 105 °C.

Characteristic features of type III T_g versus pressure behavior are the existence of a pressure maximum and a discontinuity in the slope, Figure 1. These features produce a "z-shape", including a narrow pressure region in which three glass transitions take place upon changing the temperature isobarically, e.g. at 70 bar. In contrast, a feature of type II T_g versus pressure behavior is the absence of extrema and discontinuities over this temperature range. An artificial discontinuity appears in the type II curve, since the lattice fluid theory overpredicts

* Abstract published in *Advance ACS Abstracts*, December 1, 1993.

0024-9297/94/2227-0365$04.50/0

Table 1. Polymer Characterization

polymer	wt % MMA	vol % MMA	MW_w	T_g (°C)	density (g/cm³)
PMMA	100	100	75 000	105	1.200
SMMA60	58.5	55.5		102	1.132
PS	0	0	280 000	100	1.047

the critical temperature and pressure for this set of parameters. Both types II and III have another pressure maximum at much lower temperatures (not shown).[21] Type I behavior, which is not shown in the figure, exhibits a single T_g minimum as a function of pressure.[21]

The characteristic features of the T_g versus pressure behavior shown in Figure 1 are related to the solubility of the diluent in the polymer.[18,21] For type IV behavior, the interaction between diluent and polymer is strong relative to that in types III and II. The high solubility of the diluent vapor produces a glass to liquid transition at relatively mild pressures. As the interaction between the diluent and polymer becomes less favorable, higher pressures are needed to achieve a diluent solubility required to produce a glass to liquid transition. In the case of type III behavior, these higher pressures are associated with a vapor to liquid transition of the diluent. The diluent solubility in the polymer is a much weaker function of pressure for the liquid relative to the vapor; therefore, a dramatic, discontinuous change in the T_g versus pressure behavior is observed. For type II behavior, the diluents transition from vaporlike to liquidlike behavior is continuous, as it occurs above the critical point. Hence the T_g versus pressure behavior of the polymer is continuous.

The objective of this study is to confirm experimentally novel T_g versus pressure behavior predicted by the model, specifically features of type III and II behavior. We wish to complement our earlier observation of type IV behavior for CO_2 in PMMA.[18,22] Presently, we examine poly(methyl methacrylate-*co*-styrene) and polystyrene, in order to decrease the solubility of CO_2. For instance, at 35 °C and 25 bar the solubility of CO_2 in PS is about half that in PMMA.[7] At a given temperature, lower solubility should result in higher pressures required to produce a glass to liquid transition of the polymer, as the methyl methacrylate content of the polymer is lowered. This change is expected to lead from type IV to type III and II T_g versus pressure behavior.

Experimental Section

Materials. Poly(methyl methacrylate-*co*-styrene) (Richardson Polymer, RPC 100), and polystyrene (Scientific Polymer Products, 039A) were prepared by free radical polymerization and are atactic. The copolymer is random. The physical properties of the polymers are given in Table 1 according to the manufacturer. Instrument grade CO_2 (99.99% purity) was purchased from Liquid Carbonic. Films were prepared by the solvent cast method by using dichloromethane. The solvent was evaporated at ambient conditions, and the films were dried in a vacuum oven which was heated to 20 °C above the T_g of the polymer at a rate of 20 °C/12 h. The films were between 75 and 100 μm thick.

Creep Compliance. Mechanical property measurements, specifically creep compliance, were used to determine the glass transition temperature as a function of CO_2 partial pressure. The creep compliance is defined as the strain observed for the polymer sample divided by the applied tensile stress. The apparatus and procedure have been described previously.[18] For each experiment, a 75 μm × 3.8-mm polymer strip, 4.5 cm in length, was suspended in a Jerguson sight gauge. Attached to the bottom of the polymer was a weight varying from 4 to 10 g. Following evacuation of the system, the polymer was equilibrated with a CO_2 phase. During equilibration, the polymer and weights were supported by a pan so that the polymer did not experience any tensile stress until it was equilibrated with the CO_2. The pan was lowered after equilibration, subjecting the polymer to a constant tensile stress for a period of 1 h. The reported creep compliance values were defined for a constant time of 15 min. Corrections due to polymer dilation and buoyancy were applied as described in detail elsewhere.[18] A series of creep compliance measurements were made as a function of temperature, isobarically, or as a function of pressure, isothermally. The former technique is more efficient in regions where the slope of T_g versus pressure is shallow, and the latter is preferable for regions with steep slopes.

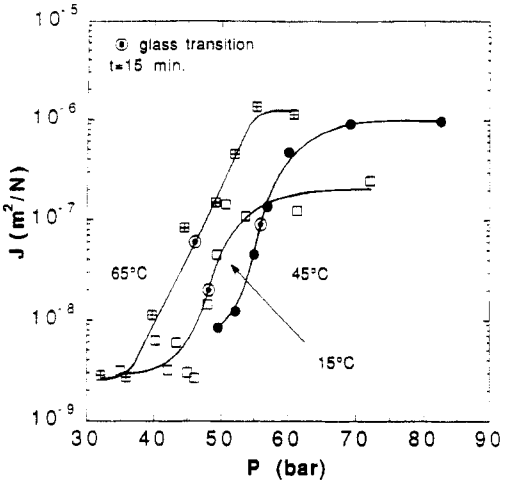

Figure 2. Creep compliance of poly(methyl methacrylate-*co*-styrene) (SMMA60) as a function of CO_2 pressure at various temperatures.

Results and Discussion

T_g versus CO_2 Partial Pressure. Figure 2 shows the creep compliance behavior of SMMA60 as a function of CO_2 partial pressure for temperatures of 65, 45, 15 °C, and a constant time of 15 min. Each isotherm has a characteristic "s-shape" behavior from the glassy, through the transition region, to the rubbery plateau. The glass transition is identified at the midpoint between the glassy and rubbery plateau regions, as indicated on the figure. The creep compliance changes several orders of magnitude in the vicinity of the glass transition. The magnitude of the creep compliance values are similar to those observed for CO_2 in PMMA.[18,22]

The glass transition pressure increases from 65 to 45 °C and then decreases from 45 to 15 °C. This behavior indicates a pressure maximum and thus retrograde vitrification. At 5 °C, no glass transition in SMMA60 is observed up to a pressure of 100 bar. This behavior indicates a small negative slope, dT_g/dP_{CO_2}, at high pressure (see Figure 1). Therefore, creep compliance measurements were performed as a function of temperature at constant pressure below 15 °C.

The creep compliance behavior of SMMA60 is shown as a function of temperature in Figure 3. Creep compliance values similar to those of Figure 2 are observed in the glassy and rubbery plateau regions. In this region, pressure has little effect on T_g compared with the behavior observed in Figure 2, because CO_2 is in the liquid state, where it is relatively incompressible.

Figure 4 shows the experimental T_g behavior as a function of pressure for SMMA60. Between 102 and 15 °C there exists a pressure maximum and thus retrograde vitrification. There is also a discontinuity in the T_g versus pressure behavior which occurs at the intersection of the CO_2 vapor pressure curve. At 15 °C, a cusp is present. The relatively low creep compliance values at 15 °C in the rubbery plateau region (see Figure 2) are caused by the

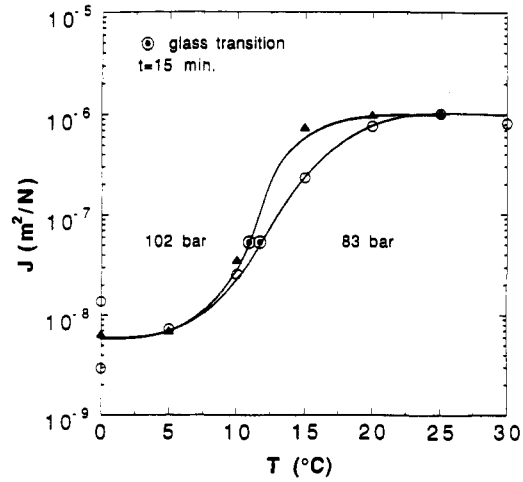

Figure 3. Creep compliance of SMMA60 as a function of CO_2 temperature at various pressures.

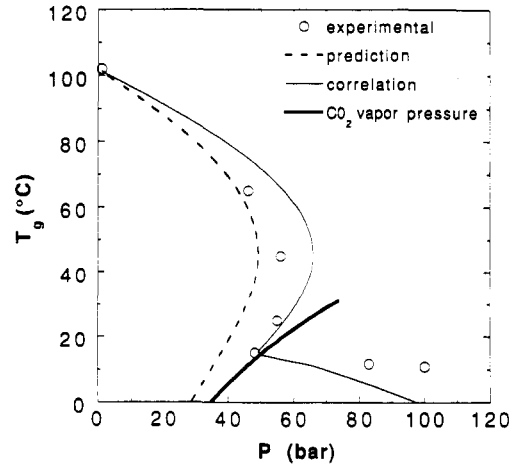

Figure 4. T_g of SMMA60 as a function of CO_2 pressure: (- - -) prediction using ζ_{12} = 1.135 obtained from solubility data; (—) correlation using ζ_{12} = 1.120 obtained from T_g data.

close proximity of the glass boundaries surrounding the cusp. The pressure maximum and discontinuity produce a "z-shape" in the T_g versus pressure behavior. This results in a narrow pressure region between about 48 and 58 bar where the polymer can experience three glass transitions upon changing the temperature isobarically. Consider a temperature of 120 °C and a pressure of 52 bar. Here the pure polymer is a liquid or a rubber above its T_g of 102 °C. Decreasing temperature isobarically results in vitrification at about 53 °C; the sorbed CO_2 causes a significant T_g depression from the pure polymer value of 102 °C. A further isobaric decrease in temperature of the glassy polymer causes the solubility of CO_2 in the polymer to increase. This solubility increase is dramatic enough to cause the polymer to experience a glass to rubber transition at about 20 °C. Isobarically, decreasing the temperature to 13 °C results in revitrification of the polymer. Therefore, the polymer experiences three glass transitions upon changing the temperature isobarically.

It is instructive to examine other regions of the experimental data in detail. Consider the pure polymer T_g of 102 °C. Decrease the temperature of the polymer to 65 °C, isobarically at 1 bar. This temperature decrease causes a decrease in thermal energy of the polymer, resulting in vitrification. Although the solubility of CO_2 increases as a result of the temperature decrease, it is insufficient to bring the polymer to the rubbery state. In this case, a pressure increase to about 46 bar is required to achieve a sufficient CO_2 concentration for the polymer to experience a glass to liquid transition. Next consider decreasing the temperature from 65 to 45 °C at a constant pressure of 46 bar. Here, as previously, the polymer is vitrified. The corresponding increase in CO_2 solubility in the polymer is insufficient to bring the polymer to the rubbery state. A further pressure increase is required to achieve sufficient CO_2 concentration to reach the rubbery state. It is important to note that the magnitude of the slope of the T_g versus pressure is increasing. That is, for a given decrease in temperature, the pressure increment required to plasticize the polymer enough to traverse a glass to rubber transition decreases. This is because the solubility of CO_2 in the polymer becomes a stronger function of both pressure and temperature as temperature decreases.[20]

Table 2. Parameters Used in Application of Condo et al. Model[21]

compd	T^* (K)	P^* (MPa)	ρ^* (kg/m³)	$\Delta\epsilon_2$[a] (J/mol)
CO_2[30]	309	574	1505	
PMMA[24]	696	503	1269	7443
SMMA60[31]	740	457	1196	7183
PS[24]	735	357	1105	7151

[a] $\Delta\epsilon_2$ values calculated in the course of this study.

Next consider a temperature decrease from 45 to 25 °C at 56 bar. Here the solubility increase due to the temperature decrease is sufficient to bring the polymer to the rubbery state. Therefore, no pressure increase is required. Decreasing temperature from 25 to 15 °C causes a further CO_2 solubility increase, resulting in an actual decrease in the pressure required to cause a glass to rubber transition of the polymer. Decreasing the temperature from 15 to 5 °C again results in vitrification. In addition, CO_2 has condensed to a liquid. As a liquid, CO_2 solubility in the polymer is a much weaker function of pressure relative to that of CO_2 vapor.[21] Therefore, for a given pressure increase, the CO_2 solubility increase in the polymer is considerably less for the CO_2 liquid relative to the vapor. Consequently, the T_g of the polymer only decreases 4 °C for a relatively large pressure increase of about 40 bar.

We now present a brief summary of a lattice fluid model developed to calculate the effect of a diluent's partial pressure and concentration on the T_g behavior of a polymer.[21] The lattice fluid equation of state and the fundamental thermodynamic criterion of equilibrium (equality of the chemical potential between phases) are used to calculate the diluent solubility in a polymer as a function of pressure and temperature.[23-27] In this calculation a binary interaction parameter, ζ_{12}, is correlated to characterize the polymer–diluent interaction strength, $\epsilon_{12}^* = \zeta_{12}(\epsilon_{11}^*\epsilon_{22}^*)^{1/2}$, where ϵ_{ij}^* is the segment energy for an i–j interaction. Given the solubility, the Gibbs–DiMarzio criterion[28-30] is used to determine the glass transition temperature of the polymer. The Gibbs–DiMarzio thermodynamic criterion states that the system entropy is zero at the glass transition.[28-30] The model does not preclude the kinetic aspect of the glass transition. A kinetic aspect is implicitly incorporated in the model by using the experimental T_g of the pure polymer to correlate a flex energy parameter of the polymer, $\Delta\epsilon_2$.[27-30] Table 2 shows the characteristic parameters for the pure components and the flex energy parameters for the polymers.[24,30,31]

The model predicts type IV T_g versus pressure behavior for the CO_2–SMMA60 system. The polymer–diluent binary interaction parameter, ζ_{12}, of 1.135 was correlated using independent CO_2 solubility data in the glassy polymer.[7] Strictly speaking, the glassy polymer is not at equilibrium and thus solubility data are not fully described by the model. The T_g data may be treated more accurately

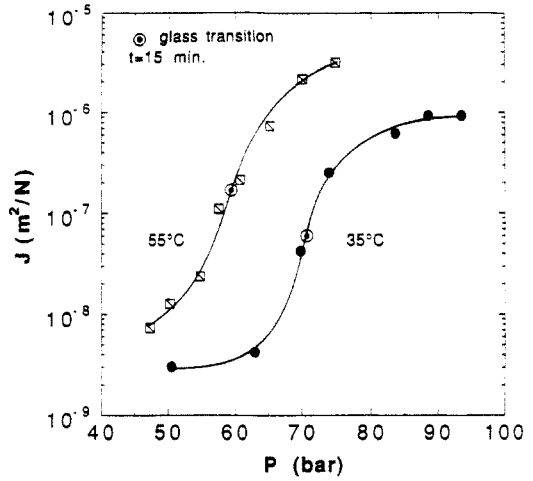

Figure 5. Creep compliance of PS as a function of CO_2 pressure at various temperatures.

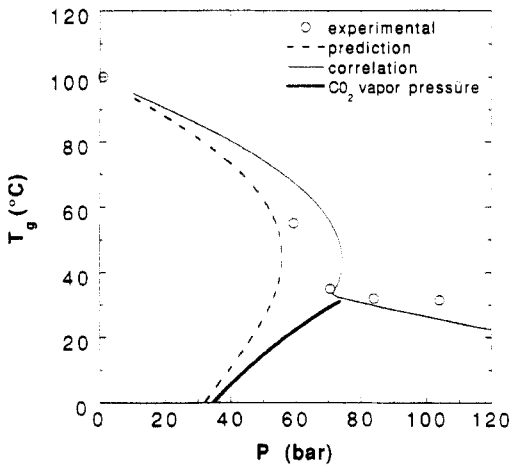

Figure 6. T_g of PS as a function of CO_2 pressure: (- - -) prediction using ζ_{12} = 1.124 obtained from solubility data; (—) correlation using ζ_{12} = 1.110 obtained from T_g data.

by correlating a new value of ζ_{12} directly from the T_g data. The complex "z-shape" of the T_g behavior is correlated successfully with a value of ζ_{12} equal to 1.120. The model depicts both the pressure maximum and discontinuity in the T_g behavior.

The creep compliance behavior of PS as a function of CO_2 pressure is shown in Figure 5. The magnitude of the creep compliance is similar to that described earlier for SMMA60. For PS, the glass transition pressure increases, as the temperature decreases. At 5 °C, the glass transition is not observed up to a pressure of 150 bar. As stated previously, this is an indication of a small negative slope, dT_g/dP_{CO_2}, at high pressure. Therefore, further creep compliance measurements were made as a function of temperature at constant pressure.

Figure 6 shows the glass transition temperature of PS as a function of CO_2 pressure. The experimental data suggest an absence of extrema or discontinuities (most likely type II behavior) in contrast to results for PMMA and SMMA60. The data are near the borderline between type II and III behavior. A great deal of experimental effort would be required to further characterize the behavior near the critical point. There is a dramatic change in the T_g behavior as a function of pressure near the critical point of the diluent. Here the chemical potential of CO_2 is a strong function of temperature and pressure, causing large changes in solubility behavior. Immediately below the critical pressure, the T_g depression is about 20 °C for a 10-bar pressure increase. However, above the critical

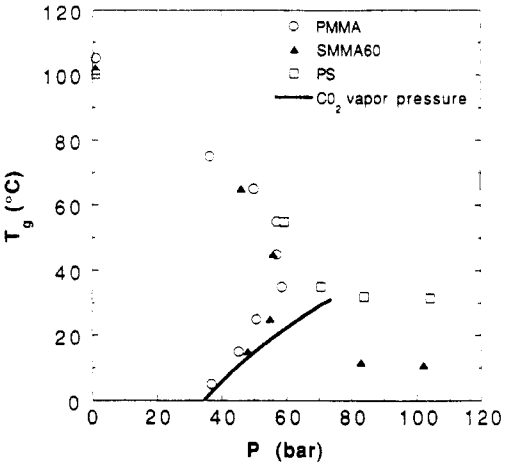

Figure 7. Summary of T_g of PMMA, SMMA60, and PS as a function of CO_2 pressure.

pressure where CO_2 is more liquidlike, a very small T_g depression of 3 °C is found for the same 10-bar pressure increase.

A previous study of the PS–CO_2 system by Wang et al.[32] which used a creep compliance technique shows a T_g minimum as a function of pressure. The data reduction procedure used the superposition principle[33] and WLF theory,[33] resulting in T_g's which can be different from the system temperature. Our T_g data at 55 and 35 °C are qualitatively similar to a more recent study by Wissinger and Paulailtis.[34] In both of these studies the T_g was determined directly from the experimental creep compliance behavior without the need to use the superposition principle or WLF theory. Excluding the study by Wang et al., we find no studies of the PS–CO_2 system that would allow us to compare our data below 35 °C.

The model predicts type IV T_g versus pressure behavior for ζ_{12} equal to 1.124, which was determined from solubility data.[35] As was the case for SMMA60, very limited solubility data for the PS–CO_2 system diminish the model's effectiveness for predictions of T_g. The T_g data may be correlated fairly well for ζ_{12} of 1.110, but agreement is limited somewhat in the near critical region. This uncertainty is because the model parameters for CO_2 do not give an accurate calculation of the vapor pressure curve near the critical point.[21] According to the model, the T_g versus pressure behavior intersects the vapor pressure curve of CO_2, resulting in a discontinuity. The model also shows incorrectly a slight pressure maximum. Despite these limitations, the model is capable of predicting the features of type II systems, as shown in Figure 1. Greater accuracy could be obtained by calculating the properties of the CO_2 phase with a highly accurate empirical equation of state.

Figure 7 shows the T_g behavior of SMMA60 and PS together with that of PMMA.[18,22] A comparison of the experimental results with those of the model in Figure 1 shows that PMMA, SMMA60, and PS exhibit features of type IV, III, and II T_g versus pressure behavior with CO_2, respectively. Therefore, features of all types of T_g versus pressure behavior proposed by the model[21] have been confirmed experimentally. Further experimentation is necessary to confirm another distinguishing feature of type II and III behavior, i.e. the pressure maximum at temperatures below those studied here.[21]

The T_g at a given pressure depends primarily upon the T_g of the pure polymer and the solubility of the diluent. The solubility depends upon general dispersion and polar interactions as well as Lewis acid–base interactions. The nonspecific interactions between CO_2 and PMMA versus

CO_2 and PS are similar; however, CO_2 interacts specifically with the basic carbonyl group.

The T_g behaviors for PMMA and SMMA60 are very similar as a function of pressure from the pure polymer T_g to 15 °C. At the higher temperatures, the pressure required to produce a glass to rubber transition of PMMA is slightly larger than that for SMMA60. The pressure required to reach the rubbery state is controlled by the stiffness of the polymer (i.e. pure polymer T_g). PMMA has a higher T_g value than SMMA60, and so a higher pressure is required to bring the polymer to the rubbery state at a given temperature. At about 35 °C, there is a crossover point where the pressure required to produce a glass to rubber transition of PMMA becomes less than that for SMMA60. As the temperature is lowered, the specific interaction between the carbonyl group (Lewis base) and CO_2 (Lewis acid) becomes more important relative to kT. Consequently, the greater solubility of CO_2 in PMMA relative to SMMA60 results in lower pressure requirements to achieve a glass transition. The pressure requirement for PMMA is lower, despite the fact that the concentration required to plasticize PMMA is greater than that for SMMA60. The data are sufficiently accurate to demonstrate the existence of the crossover point, which is also predicted by the model.[21] The experimental uncertainty in P_g is <0.2%.

Below 15 °C, there is a marked difference in the pressures required to produce a glass to rubber transition for the two polymers. Consider an isobaric temperature decrease from 15 to 5 °C at 50 bar for PMMA and SMMA60. The temperature decrease results in a CO_2 solubility increase which is greater than that required to produce a glass to rubber transition of PMMA because of the favorable diluent–polymer interaction. This, in turn, results in an actual decrease in the pressure required to bring PMMA to the rubbery state. The interaction of CO_2 with PMMA is sufficiently strong that CO_2 vapor can plasticize the polymer over the entire temperature range studied. Because the interactions of SMMA60 with CO_2 are less favorable relative to PMMA, CO_2 vapor below 15 °C cannot bring the polymer to the rubbery state. Instead, liquid CO_2 is required, typically at much greater pressures.

At high temperatures where solubilities are low and specific interactions are less important, the glass transition pressures are controlled primarily by the relative stiffness of the polymers. PMMA is stiffer than PS and has a higher glass transition pressure in this region. At lower temperatures, the donor–acceptor interaction between CO_2 and the PMMA group becomes more important. The difference in the specific interaction strengths between CO_2 and the polymer is greater for PMMA and PS than for PMMA and SMMA60. Therefore, the crossover point is reached at higher temperatures for PMMA and PS relative to PMMA and SMMA60.

T_g versus CO_2 Concentration. Figure 8 shows the complex T_g behavior as a function of pressure may be transformed to the simpler, more familiar T_g behavior as a function of diluent concentration. Higher concentrations of diluent are required to produce a glass to rubber transition as temperature decreases and the polymer loses thermal energy. The two data sets are from different experimental techniques. The data of Chiou et al.[19] are from a combination of sorption and DSC measurements. The data of Condo and Johnston are from a combination of creep compliance measurements of T_g versus P_g[18,22] and literature sorption data.[35,36] Only part of the T_g data were plotted, since the sorption data were available or could be calculated only at higher pressures.

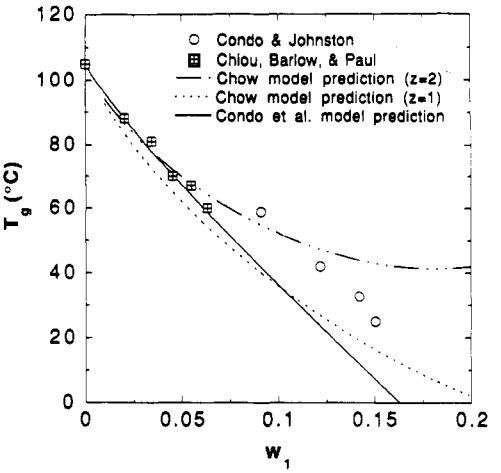

Figure 8. T_g of PMMA as a function of CO_2 concentration in weight fraction units. (The discrepancy between the two data sets is due primarily to the different definitions of the T_g, as explained in the text.)

Both data sets indicate a negative, relatively linear slope in the T_g behavior as a function of CO_2 concentration. The discrepancy between the two data sets will be shown to be due to different definitions of the glass transition, and not to the experimental technique. From mechanical property measurements of pure PMMA,[37] we obtain a T_g of 108 °C, using a tangent construction definition. The value is 3 °C larger than that measured by DSC. Therefore, the difference between the two experimental techniques for the same tangent construction definition is small compared with the discrepancy in Figure 8. Some other factor must be important.

Chiou et al.[19] used a tangent construction definition, while Condo and Johnston[18,22] used a midpoint definition. The midpoint definition yields higher glass transition pressures for a given temperature and thus higher CO_2 concentrations at the glass transition. The midpoint definition was used for the creep compliance experiments since it requires more thorough data. For the midpoint definition, the polymer must exhibit three characteristics of creep compliance behavior, specifically, glassy, transition, and rubber plateau behavior. The tangent construction definition requires that only two features be present, namely, the glassy and transition regions. If the tangent construction definition of the glass transition is employed in the creep compliance technique, the discrepancy between the two data sets is less than 1 weight %. This uncertainty is within the experimental error of the sorption measurements. Therefore, there is not a discrepancy in Figure 8, just two different definitions of T_g and modest uncertainty in sorption.

The model[21] prediction shows excellent agreement with the data obtained by the DSC technique. The model underestimates the creep compliance result by less than 3 weight %. As stated, the discrepancy between the model and the creep compliance data can be removed by employing the tangent construction definition of the glass transition. Calculated glass transition concentrations are insensitive to variation in the binary interaction parameter. Therefore, the model can successfully correlate both the pressure and concentration dependence of the glass transition temperature.

Chow developed a model which addressed the effect of diluent concentration on the T_g behavior of polymers.[38] The model was developed using lattice fluid theory[23–26] and the Gibbs–DiMarzio criterion[28,29] of the glass transition. Like the newer model,[21] the Chow model[38] has predictive capabilities and does not require knowledge of

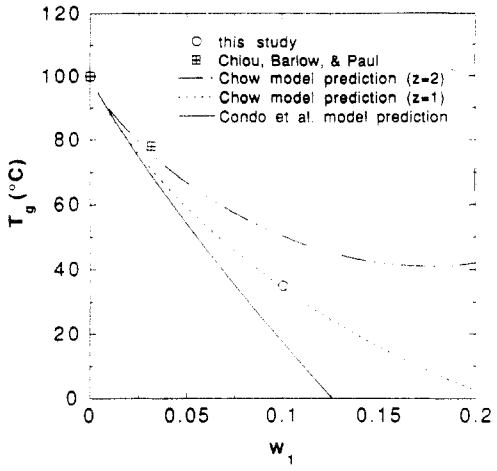

Figure 9. T_g of PS as a function of CO_2 concentration in weight fraction units.

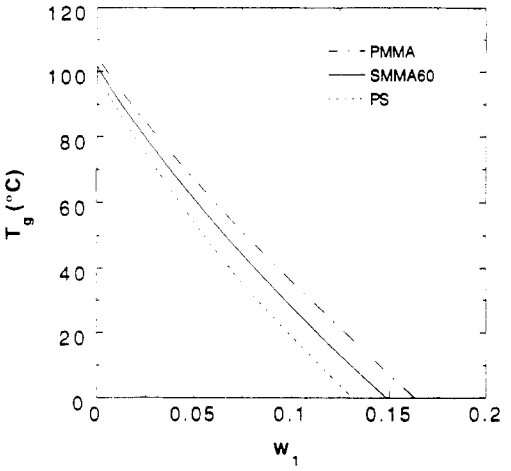

Figure 10. Model prediction of T_g of PMMA, SMMA60, and PS as a function of CO_2 concentration in the polymer in weight fraction units.

the T_g of the pure diluent. The difference between the Chow model[38] and the newer model[21] is that the new model addresses pressure, polymer flexibility, and equilibrium partitioning of the diluent explicitly.

The Chow model[38] was also applied to PMMA–CO_2 results. Parameters used in application of the Chow model are taken directly from the study of Chiou et al.[19] Using the coordination number $z = 2$, as recommended,[38] the results show a minimum in T_g as a function of CO_2 concentration. Under the conditions of this study, however, it is not expected that the T_g versus diluent concentration behavior would show a T_g minimum. Therefore, it is concluded that the Chow model performs satisfactory at low diluent concentrations, but poorly at higher concentrations.[34] It has been shown in many cases that application of the Chow model using the physically unrealistic $z = 1$ provides a better prediction of the T_g behavior as a function of diluent concentration.[19] In this case, the results show that $z = 1$ yields a more qualitatively correct result.

Figure 9 shows the T_g behavior of PS as a function of CO_2 concentration. No conclusions on model performance will be drawn since only a minimal amount of experimental data are available. The DSC data of Chiou et al. may suffer from significant CO_2 desorption losses from PS,[19] which is not the case for the new data. CO_2 desorption would shift the result of Chiou et al. isothermally to lower concentrations. The tangent construction T_g definition for the creep compliance data would also shift our result isothermally to lower CO_2 concentrations.

Figure 10 shows the model predictions for the T_g behavior of PMMA, SMMA60, and PS as a function of CO_2 concentration. As the temperature decreases, the concentration of diluent required to produce a glass to rubber transition of the polymer increases. Also, the relative concentration of the diluent required to produce a glass to rubber transition at a given temperature is directly related to the glass transition temperature of the pure polymer. As the pure polymer T_g decreases, the concentration of diluent required to take the polymer from the glassy to the rubbery state at a given temperature decreases. The T_g behavior is well-behaved as a function of diluent concentration and easily interpreted relative to the pressure behavior of the T_g which can exhibit extrema, discontinuities, and crossover points.

Conclusions

The experimental T_g results for SMMA60 and PS together with those of PMMA[18,22] confirm features of all types of T_g versus pressure behavior proposed by a recently introduced model.[21] SMMA60 exhibits a "z-shape" in the T_g behavior as a function of pressure. This feature results in a narrow pressure range where a polymer can experience three glass transitions upon changing temperature, isobarically. In contrast, PS shows no extrema or discontinuities in the T_g versus pressure behavior and therefore experiences only a single glass transition at each pressure over the extensive temperature and pressure range studied. These complex features could be correlated with the model[21] by using a single temperature independent binary interaction parameter.

The complex T_g versus pressure behavior may be transformed to the simpler, more familiar T_g behavior as a function of concentration of the diluent. As temperature decreases, thermal energy is lost by the polymer so that higher diluent concentrations are required to produce a glass to rubber transition. The model[21] is able to predict the T_g behavior as a function of diluent concentration. Also, as the pure polymer T_g decreases, the concentration of diluent required to produce a glass to rubber transition at a given temperature decreases.

A novel crossover point has been observed in the T_g behavior of polymers as a function of pressure. The crossover point is the result of a change from behavior dominated by the stiffness of the polymer to behavior dominated by the relative strength of the polymer–diluent interaction.

The complex T_g behavior versus pressure is due to the combined effects of pressure and temperature on the solubility of the diluent in the polymer. The compressibility of the diluent, which can vary dramatically throughout the vapor, liquid, and supercritical fluid conditions, has a major influence on the solubility behavior and, in turn, on the T_g behavior as a function of pressure.

Acknowledgment is made to the Separations Research Program at The University of Texas at Austin, the State of Texas Energy Research in Applications Program, and the Camille and Henry Dreyfus Foundation for a Teacher-Scholar Grant (to K.P.J.).

References and Notes

(1) McHugh, M. A.; Krukonis, V. J. *Supercritical Fluid Extraction: Principles and Practice*; Butterworths: Boston, 1986.
(2) Shim, J.-J.; Johnston, K. P. *AIChE J.* **1989**, *35*, 1097.
(3) Shim, J.-J.; Johnston, K. P. *J. Phys. Chem.* **1991**, *95*, 353.
(4) Shim, J.-J.; Johnston, K. P. *AIChE J.* **1991**, *37*, 607.

(5) Watkins, J. J.; Krukonis, V. J.; Condo, P. D.; Pradhan, D.; Ehrlich, P. *J. Supercrit. Fluids* **1991**, *4*, 24.
(6) Berens, A. R.; Huvard, G. S.; Korsmeyer, R. W. Presented at the AIChE meeting in Washington, DC, November, 1988.
(7) Raymond, R. G.; Paul, D. R. *J. Polym. Sci., Part B: Polym. Phys.* **1990**, *28*, 2079.
(8) Pope, D. S.; Koros, W. J. *Macromolecules* **1992**, *25*, 1711.
(9) Hoy, K. L.; Donohue, M. D. *Polym. Prepr. (Am. Chem. Soc., Div. Polym. Chem.)* **1990**, *30*, 679.
(10) Cha, S. W.; Suh, N. P. *Soc. Plast. Eng. Technical Conf.* **1992**, *38*, 1527.
(11) Dixon, D. J.; Johnston, K. P. *J. Appl. Polym. Sci.*, in press.
(12) Bush, P. J.; Pradhan, D.; Ehrlich, P. *Macromolecules* **1991**, *24*, 1439.
(13) Lele, A. K.; Shine, A. D. *AIChE J.* **1992**, *38*, 742.
(14) Matson, D. W.; Fulton, J. L.; Petersen, R. C.; Smith, R. D. *Ind. Eng. Chem. Res.* **1987**, *26*, 2298.
(15) Dixon, D. J.; Johnston, K. P.; Bodmeier, R. A. *AIChE J.* **1993**, *39*, 127.
(16) Tom, J. W.; Debenedetti, P. G. *Biotechnol. Prog.* **1991**, *7*, 403.
(17) Randolph, T. W.; Randolph, A. D.; Mebes, M.; Yeung, S. *Biotechnol. Prog.* **1993**, *9*, 429.
(18) Condo, P. D.; Johnston, K. P. *J. Polym. Sci., Part B: Polym. Phys.*, in press.
(19) Chiou, J. S.; Barlow, J. W.; Paul, D. R. *J. Appl. Polym. Sci.* **1985**, *30*, 2633.
(20) Kamiya, Y.; Mizoguchi, K.; Hirose, T.; Naito, Y. *J. Polym. Sci., Part B: Polym. Phys.* **1989**, *27*, 879.
(21) Condo, P. D.; Sanchez, I. C.; Panayiotou, C. G.; Johnston, K. P. *Macromolecules* **1992**, *25*, 6119.
(22) Condo, P. D.; Johnston, K. P. *Macromolecules* **1992**, *25*, 6730.
(23) Sanchez, I. C.; Lacombe, R. H. *J. Phys. Chem.* **1976**, *80*, 2352.
(24) Sanchez, I. C.; Lacombe, R. H. *Macromolecules* **1978**, *11*, 1145.
(25) Panayiotou, C. G. *Makromol. Chem.* **1986**, *187*, 2867.
(26) Panayiotou, C. G. *Macromolecules* **1987**, *20*, 861.
(27) Flory, P. J. *Proc. R. Soc. London, Ser. A* **1956**, *234*, 60.
(28) Gibbs, J. H.; DiMarzio, E. A. *J. Chem. Phys.* **1958**, *28*, 373.
(29) DiMarzio, E. A.; Gibbs, J. H. *J. Polym. Sci., Part A* **1963**, *1*, 1417.
(30) Panayiotou, C. G.; Sanchez, I. C. *Polymer* **1992**, *33*, 5090.
(31) Kim, C. K.; Paul, D. R. *Polymer* **1992**, *33*, 2089.
(32) Wang, W.-C. V.; Kramer, E. J.; Sachse, W. H. *J. Polym. Sci., Polym. Phys. Ed.* **1982**, *20*, 1371.
(33) Williams, D. L. *Polymer Science and Engineering*; Prentice-Hall: New York, 1971.
(34) Wissinger, R. G.; Paulaitis, M. E. *J. Polym. Sci., Part B: Polym. Phys.* **1991**, *29*, 631.
(35) Wissinger, R. G.; Paulaitis, M. E. *J. Polym. Sci., Part B: Polym. Phys.* **1987**, *25*, 2497.
(36) Berens, A. R.; Huvard, G. S. In *Supercritical Fluid Science and Technology*; Johnston, K. P., Penninger, J. M. L., Eds.; ACS Symposium Series 406; American Chemical Society: Washington, DC, 1989; p 207.
(37) McLoughlin, J. R.; Tobolsky, A. V. *J. Colloid Sci.* **1952**, *7*, 555.
(38) Chow, T. S. *Macromolecules* **1980**, *13*, 362.